academicJournals

Vol. 8(6), pp. 46-65, September 2017
DOI: 10.5897/JCEMS2016.0282
Articles Number: 438B1FC66341
ISSN 2141-6605

http://www.academicjournals.org/JCEMS

Journal of Chemical Engineering and Materials Science

Full Length Research Paper

Failure of Nickel-based super alloy (ME3) in aerospace gas turbine engines

A. Anvari

Department of Mechanical and Aerospace Engineering, University of Missouri-Columbia, Columbia, Missouri, U.S.A.

Received 28 December, 2016; Accepted 18 July, 2017

The significant goal of this study is to develop a system to determine the margin of safety for ME3 super alloy in aerospace gas turbine engines. This margin of safety can be defined as critical temperature, force stress, exposure time, and cycles. In this research, by applying analytical solutions and using experimental data, equations are obtained to predict the life of a nickel-base super alloy in aerospace gas turbine engines. The experimental data that are applied to obtain the equations are achieved by gas turbine environment simulation experiments. This environment is contained with mechanical cycles at high temperature. The results that are achieved by these solutions are compared with the data from an experiment on a composite material. This comparison has proved that the results of this study seem logical. Ultimately, by employing of convex, concave, and linear equations, many results to predict the life of ME3 are obtained. Main reasons in ME3 failure at gas turbine engine environment is determined by this method. Based on the results of this research, the most important cause of ME3 failure is due to maximum mechanical force at high temperatures close to 763°C.

Key words: Failure, nickel-base super alloy, gas turbine engines, mechanical fatigue, high temperature.

INTRODUCTION

Aerospace gas turbine engines are subjected to harsh environment characterized by corrosion and mechanical fatigue at high temperature. This environment can cause crack initiation and propagation. Thus, it is vital to understand the crack growth model at high temperature in gas turbine to enhance the reliability and safety (Adair, 2013).

By reviewing flight incidents caused in gas turbine engines in history, the importance of providing and improving reliability and safety of aerospace gas turbine engines is strengthened. A turbo fan engine failure on a Boeing 737 during October of 2000, due to a turbine blade chunk, turbine disk chink liberation that occurred on June 2, 2006 at Los Angeles International Airport, and an event related to turbine blade failure occurred on August 30th 2010 as Qantas Boeing 747-438 was taking off from San Francisco International Airport en route to Sydney, Australia (Adair, 2013). By considering the mentioned flight incidents, it seems that the main cause of fracture in these incidents could be due to the initiation and propagation of cracks in gas turbine engines elements.In consideration of fracture, fatigue, crack initiation and propagation, many works are presented. Among these, Yang et al. (2015) submitted “short fatigue crack growth at different maintenance times for LZ50 steel”; “fracture criterion for the tensile test of 7075 aluminum alloy” was provided by Chen and You (2015); and Xue et al. (2015) performed “long-term aging effect on the crack growth in

E-mail: aabm9@mail.missouri.edu.

the main circulating pump casing material". Furthermore, "crack growth as a function of temperature variation in carbon fiber/epoxy" and "effect of nano carbon percentage on properties of composite materials" are recently submitted by Anvari (2017, 2017a). In addition, in obtaining material properties by applying analytical methods, a few works are presented by Anvari (2016; 2017b; Adibnazari and Anvari, 2017)

According to El-Sayed (2008), materials used in the combustion chamber must tolerate a very high temperature about 2800°F due to burning gas and must be prepared to undergo the centrifugal force. An ideal material capable of withstanding such an individual condition currently in use in combustion chamber of aerospace gas turbine engines is nickel-base super alloy. This super alloy, with the combination of ceramic composite could undergo such a harsh environment.

Nickel-base super alloys mechanical properties are very appropriate to be applied in the combustion chamber of aerospace gas turbine engines like turbine discs. These unique characteristics (Gao et al., 2005) are: exceptional elevated temperature strength, high resistance to creep, oxidation, corrosion (Jiang et al., 2015), and good fracture toughness.

Many experiments have been implemented to estimate the fatigue life of gas turbine engines. Among those, "experiments and failure criteria for single crystal alloys of gas turbine engine under static and thermo cyclic loading" was submitted by Getsov et al. (2014).

Researches at NASA by implementing experiments have proved that nickel-base disk super alloy is a suitable material for gas turbine engines because it can tolerate mechanical fatigue at high temperature (Misra, 2012). Among these experiments, "determination of turbine blade life from engine field data" was provided by Zaretsky et al. (2012)

Obviously, many fatigue life predictions approaches are dependent on crack initiation and propagation. Among most works presented to estimate the fatigue life, Roy and De (2014) submit "interfacial crack problems in dissimilar bonded materials", Bhattacharjee (2013) provides "elastostatic problem of a series of collinear cracks in an orthotropic medium"; also, Anvari (2014) performs "fatigue life prediction of unidirectional carbon fiber/epoxy composite in earth orbit."

Numbers of studies and experiments to predict the maximum life time and life cycles in aerospace gas turbine engines are presented. The fatigue life, maximum exposure time, and maximum temperature allowed for applying in aerospace gas turbine engines is critically vital. It is now apparent because thousands of lives of people are spent every day in airplanes and with the advancements in aerospace industry, many new aerospace vehicles will be designed to take passengers for even farther flights. As a result, it is still necessary to predict the ME3 failure time and temperature in gas turbine engines because of safety and reliability requirements in airplanes' engines. This is of high significance because of passengers and crew lives and aerospace vehicle integrity.

In the presented study, investigation of mechanical fatigue at elevated temperatures, maximum exposure time and temperature allowed for nickel-base super alloy "ME3" in aerospace gas turbine engines with employment of experimental data (Gao et al., 2005; Misra, 2012; Anvari, 2014; Gabb et al., 2002; Gabb et al., 2009; Assoul et al., 2008), giving rise to analytical solutions. The results of analytical method can contribute to an improvement of the safety and reliability of aerospace gas turbine engines including nickel-base super alloy, ME3.

EXPERIMENTAL PROCEDURES

An advanced powder-metallurgy nickel-based superalloy ME3, was used in this study. It is a relatively new polycrystalline Ni-Co-Cr alloy, of proprietary chemical composition (similar to Udimet 720), designed to have extended durability at 650°C for aircraft engine disk applications by utilizing a moderately high precipitate content with high refractory element levels. Forged heats of the alloy were received as plate stock from General Electric (GE) Aircraft Engines (fine-grained sample) and from NASA- Glenn (coarse-grained sample). The as-received microstructure comprised a bimodal distribution of -20 nm fand 100 to 200 nm ordered (L12) precipitates within the equiaxed matrix as described by Nembach and Neite (1985). The matrix grain size (dg), was 1.3 and 15 µm in the two as-received conditions for the GE and NASA heats, respectively (Gao et al., 2005).

Twelve scaled-up baseline ME3 disks were either subsolvus or supersolvus solution heat treated. They were then removed for brief fan air-cooling followed by oil quenching. Subsequent stress relief heat treatment and aging heat treatment steps were then applied. These disks each had an outer diameter of near 24 in., maximum bore thickness of near 4 in. and rim thickness of near 2 in (Gabb et al., 2002).

Tensile tests: Machining and testing of scaled-up disk tensile specimens was performed by Dickson Testing Company. Specimens having a gage diameter of 0.25 in. and gage length of 1.25 in. were machined and then tested in uniaxial test machines employing induction heating and axial extensometers. The tests were performed according to ASTM E21, using an initial test segment with strain increased at a uniform rate of 0.2%/min., followed by a segment with increased displacement at a uniform rate of 0.2 in./min (Gabb et al., 2002).

Low cycle fatigue tests: Machining from scaled-up disks of low cycle fatigue specimens having gage diameters of 0.4 in. and gage lengths of 1.25 in. was performed *by* BITEC CNC Production Machining. The low cycle fatigue (LCF) specimens were then tested at Mar-Test, Inc. using uniaxial closed-loop servo-hydraulic testing machines with induction heating and axial extensometers. Tests were performed according to ASTM E606" (Gabb et al., 2002).

Fatigue crack growth tests: Machining of surface flaw fatigue crack growth specimens from scaled-up disks was performed by Low Stress Grind, Inc. Machining of specimens of the same configuration from subscale disks was performed by BITEC. All specimens had a rectangular gage section 0.4 in. wide and 0.18 in. thick, with a surface flaw about 0.014 in wide and 0.007 in deep

Table 1. ME3 Mechanical properties.

S/N	Mechanical properties	Numerial value
1	Ultimate Strain, ε_f (Gabb et al., 2002)	0.15
2	Elastic Modulus, E (GPa) (Sawant et al., 2008)	246
3	Tensile Strength, S_t (MPa) (Gao et al., 2007)	1650
4	Poisson's Ratio, v	0.3
5	Shear Modulus, G (GPa)	94.6154

produced by electro discharge machining. The fatigue crack growth specimens were then tested at NASA GRC (Gabb et al., 2002).

According to NASA experimental research related to measuring the fatigue life of aerospace gas turbine engines due to mechanical fatigue at elevated temperatures, useful data are obtained. Some of these results are both achieved at 204 and 704°C with strain mechanical fatigue cycles at 0.5 and 0.75%, respectively (Gabb et al., 2009).

While disk rim temperatures approach 700°C, salt particles from air intake, engine elements, and combustion could melt (Gabb et al., 2009). The liquid salt mixture then passes through the disk surfaces and could cause corrosion damage especially at high temperatures around 700°C. Based on this procedure and experimental data by NASA (Gabb et al., 2009), it can be observed that at 704°C and strain mechanical cycles of 0.75%, the fatigue life cycles are decreased with comparison to 204°C and strain mechanical fatigue cycles at 0.5% experiment. Thus, it is a more critical condition for aerospace gas turbine engines. Due to the fact in this research, the analytical solutions provided for predicting the maximum time and temperature allowed for nickel-base super alloy "ME3" is adjusted to this condition except the condition for crack initiation life that is mentioned in the following part of the paper.

ME3 microstructure

The material ranged in average grain size from 25 to 34 µm, and as-large-as grain size of 90 to 170 µm. Mean diameters for secondary gamma prime precipitates ranged from 0.19 to 0.33 µm, and for tertiary gamma prime precipitates ranged from 18 to 39 nm. These differences in specimen microstructure were due to varying prior location of specimens from within disks, which had been given intentionally varied solution to quench heat treatments. Specimens for each test condition were selected from multiple disks and locations to span this range of microstructure, and associated mechanical response" (Gabb et al., 2009).

Supersolvus heat-treated scaled-up material had a mean grain size of ASTM 7.1 (27.5 µm), with a standard deviation of ASTM 0.2 (2.0 µm) and ALA grain size rating of ASTM 3.25. Subsolvus heat treated scaled-up material had a mean grain size of ASTM 12.0+/-0.1 (5+/-0.2 µm) and ALA grain size of ASTM 8. Within the grains of supersolvus specimens, three populations of y' precipitates were evident. Scattered large precipitates (0.3-0.5 µm diameter) appeared to have preferentially grown at the cube corners, giving consistently oriented star shapes. Selected area diffraction pattern analyses indicated the cube sides corresponded to {001} planes, while the extended cube corners grew out in <111> directions. Intermediate size precipitates (0.15-0.3 µm diameter) had a simpler, rounded cube shape. Fine precipitates (0.01-0.05 µm diameter) were spherical. Subsolvus specimens had less distinct differences in large versus intermediate precipitate morphology and size ranges, but still displayed some evidence of preferential growth at the cube corners. The fine spherical precipitates were somewhat smaller in subsolvus specimens. Coarse, undissolved "primary" y' particles (0.6-2 µm in diameter) were spaced along grain boundaries and sometimes widely scattered within grains" (Gabb et al., 2002).

PROBLEM FORMULATION

ME3 crack initiation life

Here, the crack initiation life "$2N_f$" is defined by the Manson Coffin formulation (Assoul et al., 2008). In the following equation, E is the ME3 elasticity modulus, σ_f is ME3 strength, b is equal to -0.12 (Assoul et al., 2008), and c is equal to 0.6 (Assoul et al., 2008). The strain range, $\Delta\varepsilon$, is equal to 0.5% (Gabb et al., 2009), ME3 strength, σ_f: 1650 Mpa (Gao et al., 2007), elasticity modulus, E: 246 GPa (Sawant et al., 2008), and the ME3 strain strength, ε_f, is 0.15 (Gabb et al., 2002). ME3 mechanical properties are indicated in Table 1.

$$(\Delta\varepsilon / 2) = (\sigma_f / E)(2N_f)^b + \varepsilon_f (2N_f)^c . \quad (1)$$

By substituting this mentioned numerical values into Equation 1, cycles to crack initiation (Basan et al., 2010), $2Nf=17620$, is obtained. Based on this solution, it is necessary to take serious caution after the crack initiation in order to prevent crack propagation especially at harsher environment such as higher temperature, greater stress, or both of these conditions together. After the crack initiation, the aerospace gas turbine engines are subjected to damage and in continuation with this environment, the cracks could propagate. At worse environmental conditions, such as higher temperatures or greater centrifugal forces or both of them, the cracks propagation may be faster and can even result in instant failure at gas turbine engines.

ME3 fatigue life in gas turbine

In this part of the research, equations that are applied to predict the thermo-mechanical fatigue life of unidirectional carbon fiber/epoxy composite (UCFEC) are presented. These equations are submitted by Liu and Nairn (1990). By using these equations, predicting the fatigue life of ME3 in gas turbine engine seems possible. In this study, to obtain the numerical values from these equations, all the laminas are assumed ME3.

In Equations 2 to 17 (Liu and Nairn, 1990), E_A, E_T, T_s, and T_0 are the axial moduli, transverse moduli, specimen temperature, and stress free temperature (uncracked) of ME3 super alloy. $\Delta\alpha=\alpha_T-\alpha_A$ is difference between the transverse and longitudinal thermal expansion coefficients of ME3 and $T= T_s- T_0$. p, q, α, β, and constants C_1 to C_4, are functions of mechanical properties and thicknesses of the ME3 plies: t_1 is equal to 0.25 of thickness of ME3 and t_2 is another 0.25 of ME3 thickness; such that in this research, both of them offer the same mechanical properties. Also, $h=t_1+t_2$ as shown in Figure 1 (Liu and Nairn, 1990). In Figure 2, (Maciejewski,

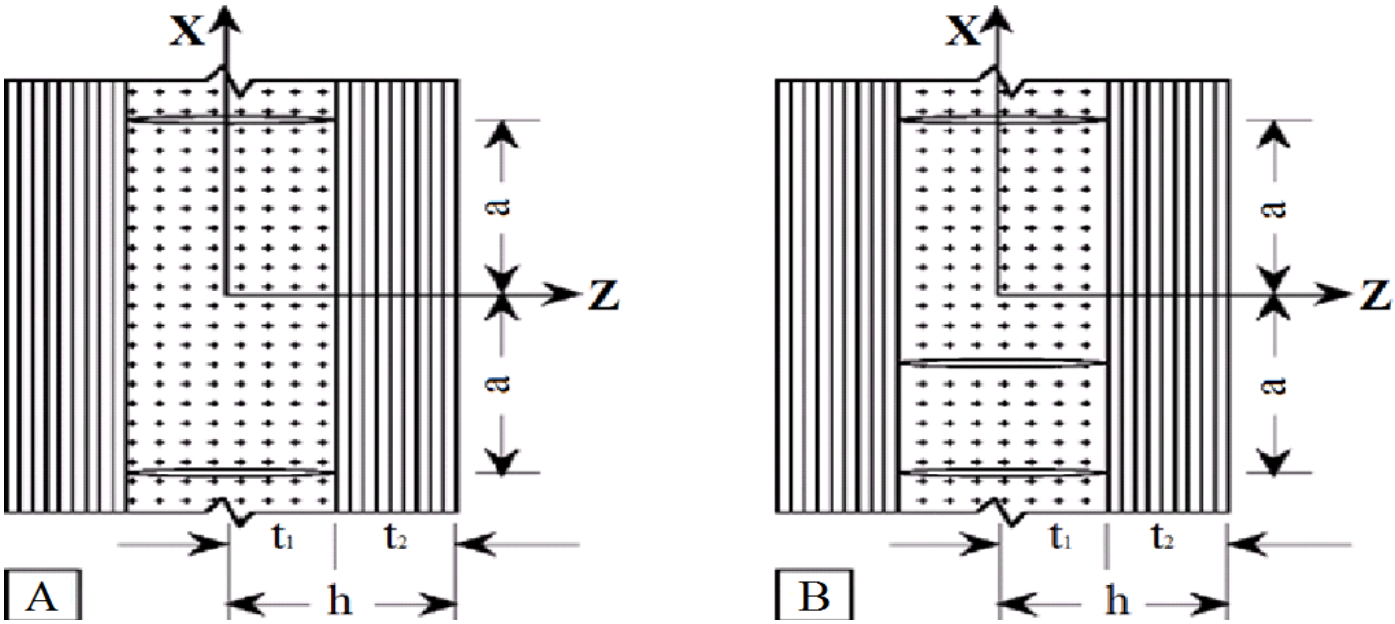

Figure 1. Edge view of UCFEC with microcracks. A: Two microcracks. B: The formation of a new microcrack (Liu and Nairn, 1990).

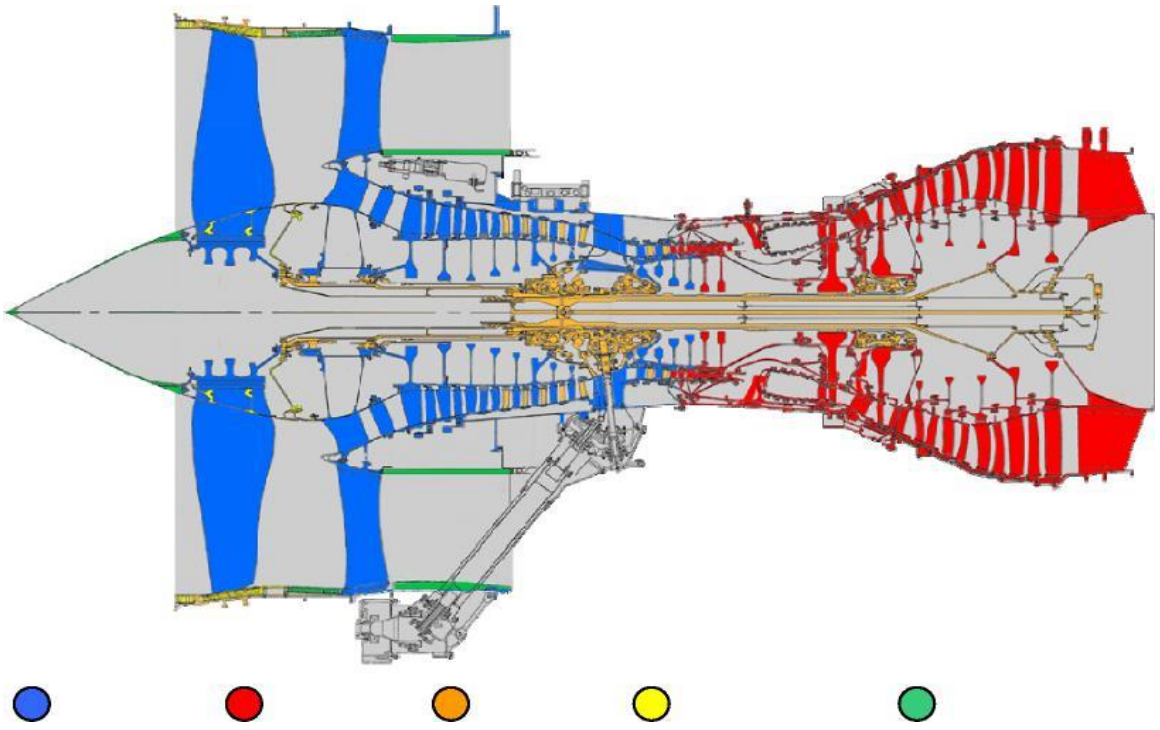

Figure 2. Common materials in a gas turbine engine (blue: Titanium, red: Nickel, orange: Steel, yellow: Aluminum, green: Composites) (Maciejewski, 2013).

2013) and 3 (Adair, 2013), gas turbine engine including ME3 (Nickel-base super alloy) is illustrated and ME3 chemical composition is indicated in Table 2. Furthermore, in Figure 3, basic turbojet gas turbine engine, which contains ME3 super alloy, is illustrated.

$$C_1 = \frac{hE_0}{t_2 E_A E_T}, \qquad (2)$$

Table 2. ME3 Chemical composition (Winston and Brooks, 2008).

Alloy	Ni	Fe	Co	Cr	Mo	W	Ta	Al	Ti	Nb	Zr	Hf	C	B
ME3	Bal	---	18.2	13.1	3.8	1.9	2.7	3.5	3.5	1.4	0.05	---	.03	.03

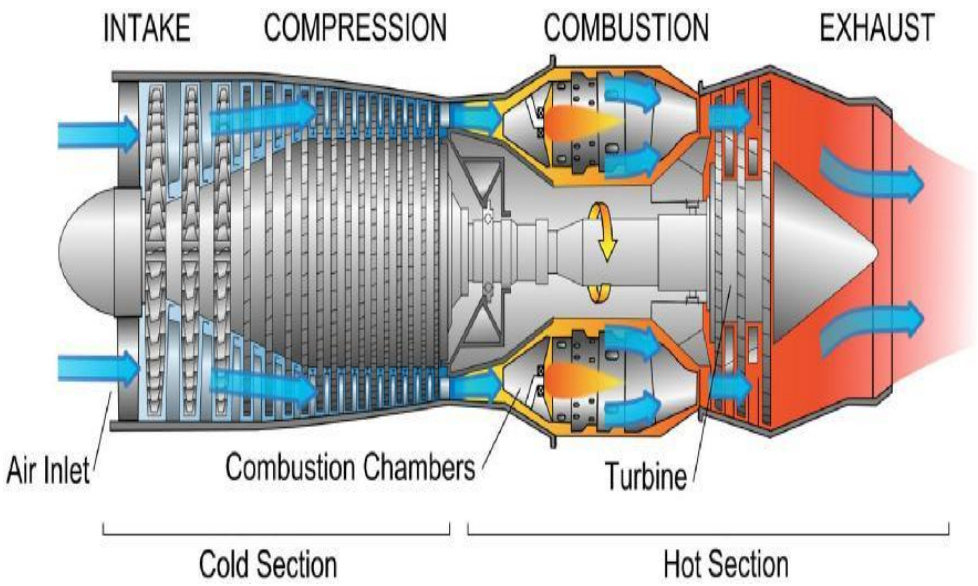

Figure 3. Schematic of a basic turbojet gas turbine engine (Adair, 2013).

$$C_2 = \frac{v_T}{E_T}(\lambda + \frac{2}{3}) - \frac{\lambda v_A}{3E_A}, \quad (3)$$

$$\lambda = \frac{t_2}{t_1}, \quad (4)$$

$$C_3 = \frac{\lambda + 1}{60E_T}(3\lambda^2 + 12\lambda + 8), \quad (5)$$

$$C_4 = \frac{1}{3}(\frac{1}{G_T} + \frac{\lambda}{G_A}), \quad (6)$$

by using C_1 to C_4, p and q are

$$p = (C_2 - C_4) / C_3, \quad (7)$$

$$q = C_1 / C_3. \quad (8)$$

Also by applying p and q, α and β are

$$a = \frac{1}{2}\sqrt{2\sqrt{q} - p}, \quad (9)$$

$$b = \frac{1}{2}\sqrt{2\sqrt{q} + p}. \quad (10)$$

These numerical values are indicated in Table 2.

G_A, G_T, v_A, and v_T, are the axial and transverse shear moduli and Poisson's ratio respectively. B=2h, is ME3 total thickness, W is the specimen width (y-direction dimension), L is the sample length (x-direction dimension), and, 2a, is the distance between 2 cracks and, C_W, is the width of each crack that in this study is assumed 5e-5 m. This study offers that B_1=0.5 mm, B_2=6 mm, and L=24 mm. The presented solution is valid for $4q/p^2$>1. By applying the present numerical values, all the results obtained from the Equations 2 to 17 (Liu and Nairn, 1990) are indicated in Tables 3 and 4. New function, $\chi(\rho)$, is

$$\chi(\rho) = 2\alpha\beta(\alpha^2 + \beta^2)\frac{\cosh 2\alpha\rho - \cos 2\beta\rho}{\beta \sinh 2\alpha\rho + \alpha \sin 2\beta\rho}, \quad (11)$$

$$\rho = (a / t_1). \quad (12)$$

$$G_m = \left(\frac{E_T}{E_c}\sigma_0 - \frac{\Delta\alpha T}{C_1}\right)^2 C_3 t_1 \, \mathrm{Y}(D), \quad (13)$$

Table 3. ME3 characteristics obtained from Equations 2 to 25, with 0.5 mm thickness and 24 mm length at 704°C (Gabb et al., 2009), ε=3.75e-3 (Gabb et al., 2009), and E=246 GPa (Sawant et al., 2008) in gas turbine engine simulation experiment.

N Cycles	a_c (mm)	N_c (-)	*a* (mm)	G_m (J/m^2)	da_c/dN (mm/Cycle)
300	0.12	3	3.0000	1.09860e-6	3.8e-4
400	0.16	4	2.4000	1.09862e-6	3.9e-4
500	0.20	4	2.4000	1.09862e-6	4.0e-4
1000	0.40	8	1.3333	1.09840e-6	4.5e-4
1500	0.65	13	0.8571	1.09121e-6	5.0e-4
2000	0.90	18	0.6316	1.05924e-6	5.5e-4
3000	1.50	30	0.3871	8.71984e-7	6.5e-4
4000	2.20	44	0.2667	6.08081e-7	7.5e-4
5000	4.40	88	0.1348	1.79828e-7	8.5e-4

Table 4**.** ME3 characteristics obtained from Equations 2 to 25, with 6 mm thickness and 24 mm length at 704°C (Gabb et al., 2009), ε=3.75e-3 (Gabb et al., 2009), and E=246 GPa (Sawant et al., 2008) in gas turbine engine simulation experiment.

N (Cycle)	a_c (mm)	N_c (-)	*D* (mm^{-1})	*a* (mm)	G_m (J/m^2)	da_c/dN (mm/Cycle)
100	0.04	1	0.083	6.0000	1.20e-5	3.600e-4
250	0.10	2	0.125	4.0000	9.30e-6	3.750e-4
300	0.12	3	0.167	3.0000	6.70e-6	3.800e-4
500	0.20	4	0.208	2.4000	4.75e-6	4.000e-4
750	0.30	6	0.292	1.7143	2.45e-6	4.250e-4
1000	0.40	8	0.375	1.3333	1.37e-6	4.500e-4
1250	0.50	10	0.458	1.0909	8.23e-7	4.750e-4
1500	0.65	13	0.583	0.8571	4.32e-7	5.000e-4
1750	0.80	16	0.708	0.7059	2.51e-7	5.250e-4
1875	0.85	17	0.750	0.6667	2.10e-7	5.375e-4
2000	1.00	20	0.875	0.5714	1.38e-7	5.500e-4
2500	1.20	24	1.042	0.4800	8.30e-8	6.000e-4
2750	1.50	30	1.292	0.3871	4.40e-8	6.250e-4
3000	1.65	33	1.417	0.3529	3.38e-8	6.500e-4
3500	2.00	40	1.708	0.2927	1.96e-8	7.000e-4
3750	2.10	42	1.792	0.2791	1.65e-8	7.250e-4
3875	2.15	43	1.833	0.2727	1.58e-8	7.375e-4
4000	2.20	44	1.875	0.2667	1.43e-8	7.500e-4
4500	3.20	64	2.708	0.1846	8.60e-9	8.000e-4
5000	4.35	87	3.667	0.1364	2.65e-9	8.500e-4
6000	7.60	152	6.375	0.0784	-1.40e-8	9.500e-4

where G_m (J/m^2) is energy release rate and Y(D) is a calibration function that depends on the crack density, D (mm^{-1}). The calibration function (Liu and Nairn, 1990) is

$$Y(D) = 2\chi(\rho/2) - \chi(\rho). \quad (14)$$

$$\frac{dD}{dN} = A\Delta G_m^n, \quad (15)$$

and before the crack forms

$$D = \frac{N_c}{L}, \quad (16)$$

also, after the crack forms

$$D = \frac{N_c + 1}{L}. \quad (17)$$

Where N_c, a_c, and C_W, are the crack numbers, crack length, and crack width in sample.

$$N_c = a_c / C_W. \quad (18)$$

It is proposed to analyze fatigue data using a modified Paris-law approach in which the rate of change in microcrack density is given by Equation 15, where A and n are two power-law fitting

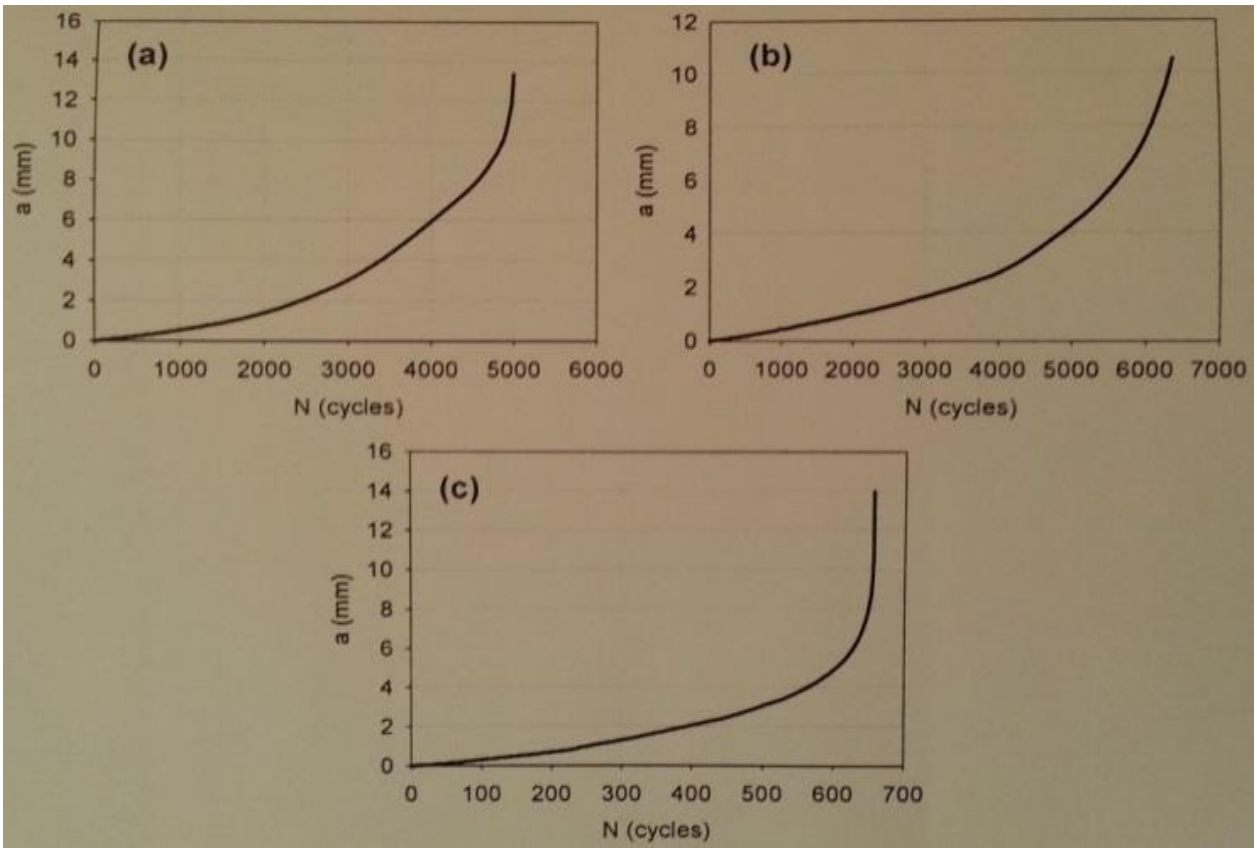

Figure 4. Typical crack length, a_c (mm), versus number of cycles, N for (a) 650°C, (b) 704°C and (c) 760°C (Maciejewski, 2013).

parameters. The conventional Paris-law approach relates the rate of change in crack length to the range in the applied stress intensity factor-Δ K. In the microcracking fracture experiment, the stress intensity factor approach is not possible and therefore substituted ΔG for ΔK (Liu and Nairn, 1990).

Based on this research, for ME3 sample, $\Delta\alpha=\alpha_T-\alpha_A$ is equal to zero and $E_T=E_C$, so G_m formulation changes into

$$G_m=\sigma_0 C_3 t_1 \mathrm{Y}(D), \tag{19}$$

that is equal to

$$G_m=Ee\, C_3 t_1 \mathrm{Y}(D). \tag{20}$$

As mentioned, E and ε are 246 GPa (Sawant et al., 2008) and 0.75% (Gabb et al., 2009) respectively. Thus, the numerical value of G_m can be obtained by using the presented data and functions in this research.

In Figure 4b (Maciejewski, 2013), ME3 crack length as a function of mechanical cycles in gas turbine engine simulation experiment at 704°C is illustrated. By using this data, an equation to obtain the crack length as a function of cycles is feasible. With this equation, and by applying partial derivative, obtaining the crack density growth rate is possible.

$$a_c = aN^2 + bN + c. \tag{21}$$

At the beginning of the simulation experiment (0 cycle), the crack length is equal to zero, so

$$0 = a(0)^2 + b(0) + c, \tag{22}$$

and at 2000 cycles, crack length is equal to 0.9 mm, so

$$0.9 = a(2000)^2 + b(2000) + c, \tag{23}$$

also in 4000 cycles, the crack length in sample is, 2.2 mm. As a result

$$2.2 = a(4000)^2 + b(4000) + c. \tag{24}$$

Therefore, by solving three Equations ((22), (23), and (24)), three unknown quantities (a, b, and c), Equation (25) is obtained. This equation indicates the ME3 sample crack length as a function of cycles in gas turbine engine at 704°C. This function is also illustrated in Figure 5.

$$a_c = (5e-8)(N^2) + (3.5e-4)(N). \tag{25}$$

$$\frac{da_c}{dN} = (1e-7)N + 0.00035. \tag{26}$$

Figure 5. Crack length in ME3 sample as a function of cycles in gas turbine engine simulation experiment at 704°C.

All the data for obtaining the equations numerical values (Equations 2 to 20) are now available. So, by substituting the information in the equations, the numerical values are indicated in Tables 3 and 4.

In Figures 6 to 8 (Adair, 2013), 7 (Maciejewski, 2013), and 8 (Zaretsky et al., 2012), gas turbine engine failure due to existing of thermo-mechanical fatigue (TMF) cracks in turbine disk and blades are illustrated. The material that is used in the hot section of gas turbine engines is nickel-base super alloy (Zaretsky et al., 2012). In present and previous parts of the paper, the crack initiation and propagation process due to thermo-mechanical fatigue is explained.

CONVEX, CONCAVE, AND LINEAR FUNCTIONS METHOD

The objective here and subsequently is to use experimented results data as boundary conditions to develop equations that can estimate the maximum life and temperature allowed in ME3 super alloy in gas turbine engines. The maximum life and temperature obtained by these equations can be used to establish a margin of safety for ME3 super alloy in aerospace gas turbine engines environment.

In order to better understand the convex, concave, and linear functions method, it is worth mentioning that for developing any convex or concave curve, three boundary conditions or points from experiments on ME3 super alloy are required. Moreover, in order to develop a linear function, two boundary conditions or points from experiments on ME3 super alloy in aerospace gas turbine engines environment are required. In addition, for applying these equations, it is enough to make these equations equivalent to the values of ME3 super alloy properties. As an example, in Table 6, if Equation 27 is equal to yield strength of ME3 super alloy, as a result, the obtained temperature from Equation 27 is the temperature related to the yield strength of ME3 super alloy. It means at this temperature ME3 is yielded. Thus, it is recommended that ME3 does not apply at this temperature or higher temperature than this because in this estate, ME3 would yield and deform. Hence, it may crash to other pieces in engines such as body and blades. As a result, it is not safe to use.

All of the following equations can also be interpreted with this methodology. After all of the equations are solved by equalization to ME3 properties values as mentioned in example, maximum life and temperature allowed to be obtained can be applied as the margin of safety. For more safety, minimum results are accepted.

This approach is applied in the following sections for determining fatigue, strength, durability, and temperature limit of ME3 super alloy in aerospace gas turbine engines.

Fine and course ME3 yield and ultimate strength as a function of temperature

In Table 5 (Gao et al., 2005), experimental results in order to determine the fine and course ME3 yield and ultimate strength at different temperatures are available. By applying these data, four functions to determine yield and ultimate strength at different

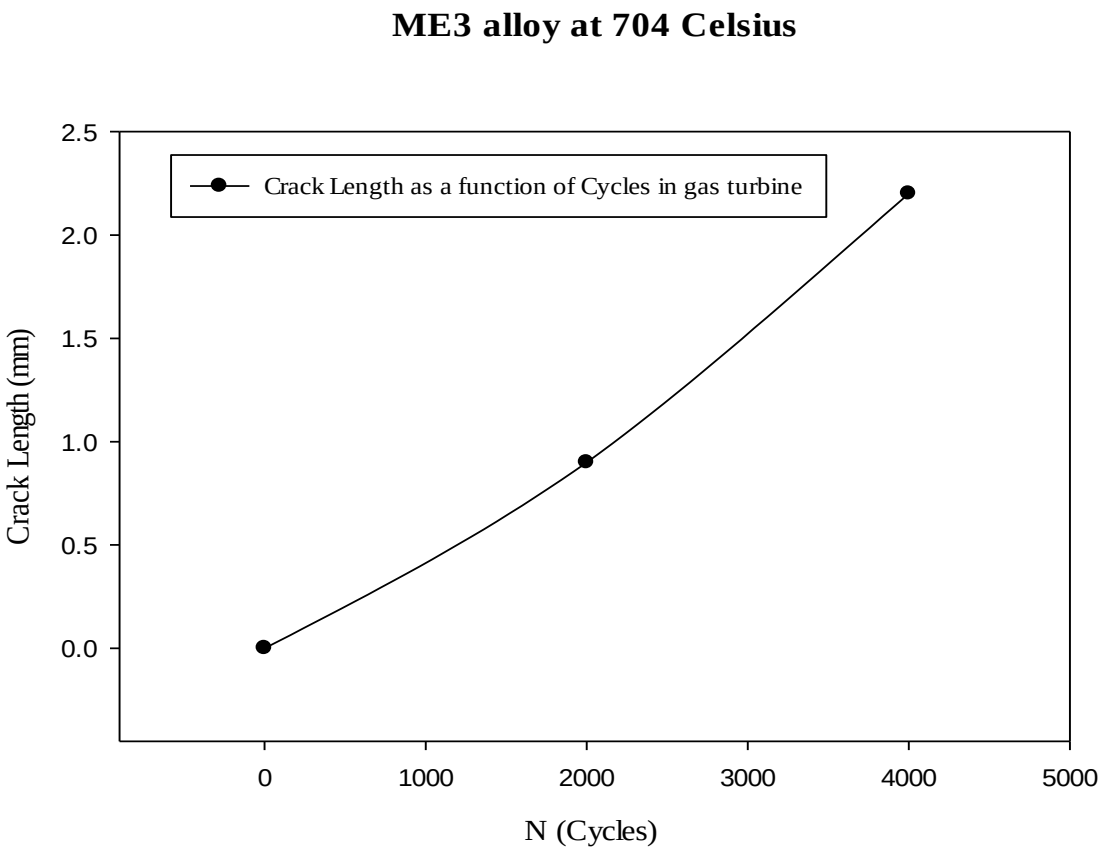

Figure 6. Turbofan engine blade failure: (bottom) fractured blade toot (top) perforated engine nacelle (Adair, 2013).

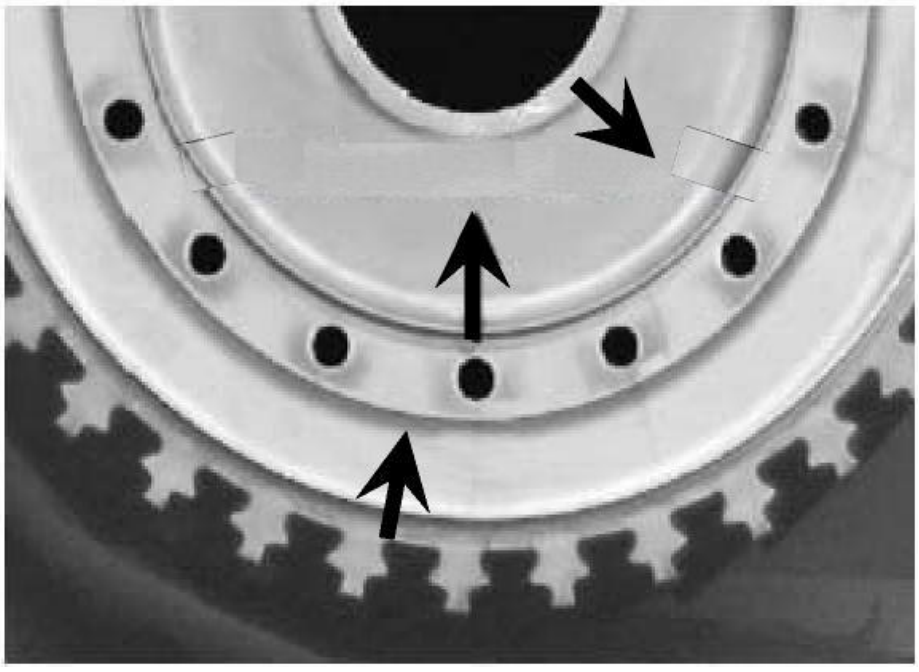

Figure 7. Typical cracking locations in the turbine disk, where the arrows indicate the cracking direction (left figure) (Maciejewski, 2013).

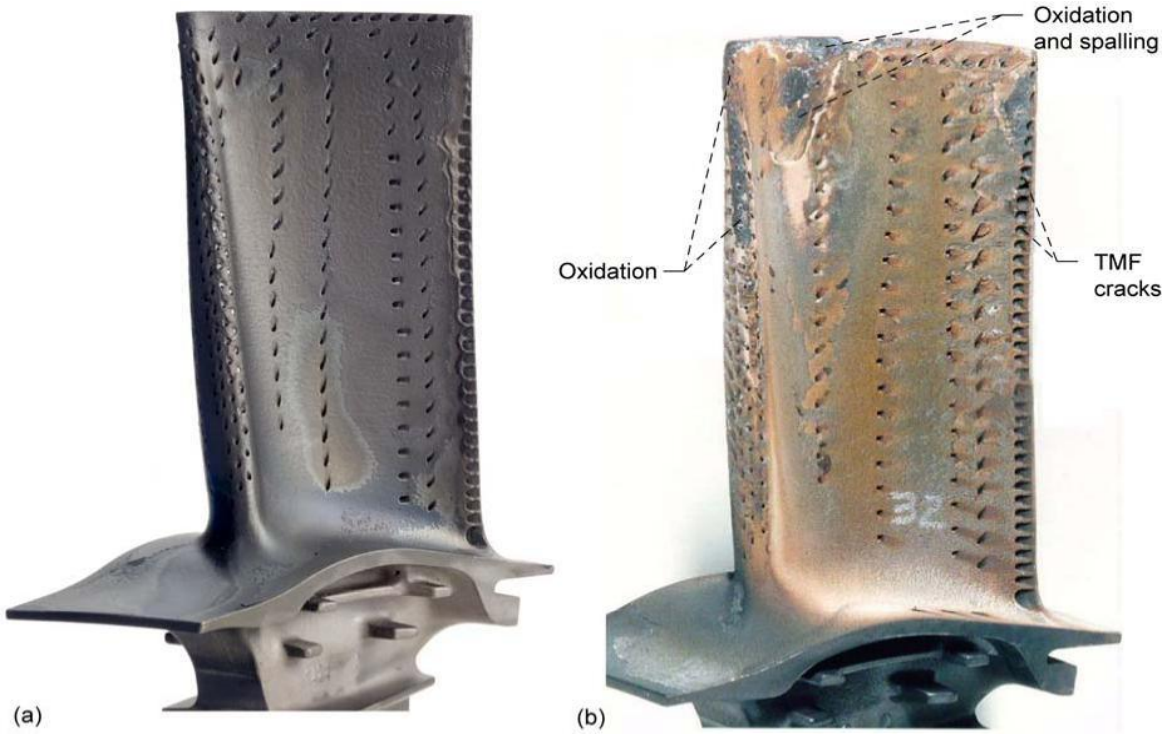

Figure 8. Comparison of unfailed and failed T-1 turbine blades used in study. Example of (a) unfailed T-1 turbine blade (b) failed T-1 turbine blade (right figure) (Zaretsky et al., 2012).

Table 5. Typical mechanical properties of the as-received ME3 alloy at ambient and elevated temperature for the initially fine-grained and coarse- grained heats (Gao et al., 2005).

Temperature (°C)	Yield Strength (MPa)	Ultimate Strength (MPa)	Reduction in Area (%)
25 (fine)	1180	1620	26
700 (fine)	1040	1300	18
25 (coarse)	1150	1650	21
700 (coarse)	980	1310	15
800 (coarse)	900	980	12

temperatures are obtained by using the method used to develop the Equation 25. These functions are indicated in Table 6.

ME3 ultimate and tensile strength

According to Figures 9 and 10, ultimate and tensile strength of ME3 super alloy are functions of temperature variation. In Figure 9 (Winston and Brooks, 2008), there are three boundary conditions to develop a curve in order to determine the ultimate strength as a function of temperature. Also, in Figure 10 (Winston and Brooks, 2008), there are three points to create a function. These equations are shown in Table 7.

ME3 Fatigue life as a function of temperature

Figures 11 and 12 (Misra, 2012) are contained with numbers of information about the ME3 super alloy at different time and temperature. These data are collected and listed in Table 8; furthermore, by using these data equations, the fatigue life cycles as functions of time and temperature are predicted in Table 8. It is important to notice that in these figures, it is obvious that at 24 h and before it there are remaining life cycles. Based on this logical fact, the ME3 maximum lifetime at 704°C is always more than 24 h. Thus, the results more than 24 h are “accepted” and the results less than 24 h are “not accepted”. Due to caution from the results obtained, always the minimum results are “accepted”. Thus, the minimum results that are more than 24 hours are accepted. This logic is used in different parts of this study as applied in Table 8.

ME3 fatigue life at gas turbine engine maximum force

There are three curves in Figure 4 (Maciejewski, 2013), viz; crack length as a function of cycles at 650, 704 and 760°C. In each of the curves, a, b, and c, in an individual cycle number, the crack length grows rapidly. These cycle numbers are the end of fatigue life for ME3

Table 6. Equations obtained from the data in Table 5 to indicate the fine and course ME3 yield and ultimate strength as a function of temperature.

ME3 Condition	Boundary Conditions (Gao et al., 2005)	Equation
Fine	(T=25°C, S_y=1180 MPa) and (T=700°C, S_y=1040 MPa)	-0.2074(T)+1185.1852=S_y, (27)
Fine	(T=25°C, S_u=1620 MPa) and (T=700°C, S_u=1300 MPa)	-0.4741(T)+1631.85185=S_u, (28)
Course	(T=25°C, S_y=1150 MPa), (T=700°C, S_y=980 MPa), and (T=800°C, S_y=900 MPa)	-0.00071(T^2)+0.26285(T)+1143.8725= S_y, (29) *Convex Curve*
Course	(T=25°C, S_u=1650 MPa), (T=700°C, S_u=1310 MPa), and (T=800°C, S_u=980 MPa)	-0.00361(T^2)+2.11222(T)+1599.45083= S_u, (30) *Convex Curve*

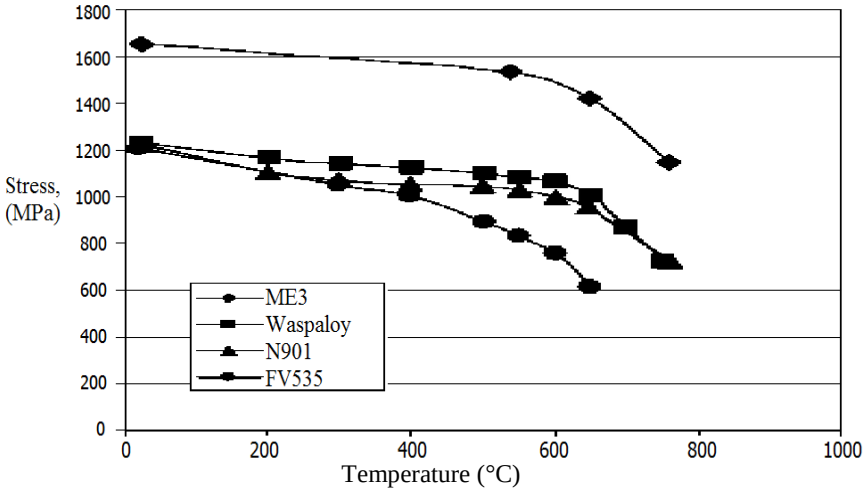

Figure 9. Ultimate strength of typical disc alloys (Winston and Brooks, 2008).

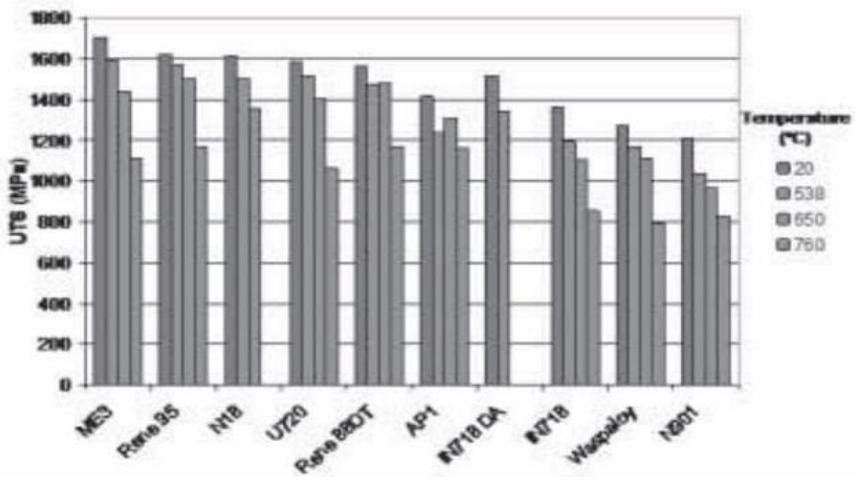

Figure 10. Tensile strength of some Ni disc alloys (Winston and Brooks, 2008).

Table 7. ME3 ultimate and tensile strength equations as functions of temperature variation.

ME3 Boundary Conditions (Winston and Brooks, 2008)	Equation
(T=25°C, S_u=1650 MPa), (T=535°C, S_u=1540 MPa), and (T=760°C, S_u=1150 MPa)	-0.002065(T^2)+0.94057(T)+1627.7764=S_u, (31) *Convex Curve*
(T=20°C, S_t=1700 MPa), (T=650°C, S_t=1430 MPa), and (T=760°C, S_t=1105 MPa)	-0.00341(T^2)+1.85847(T)+1664.1946= S_t, (32) *Convex Curve*

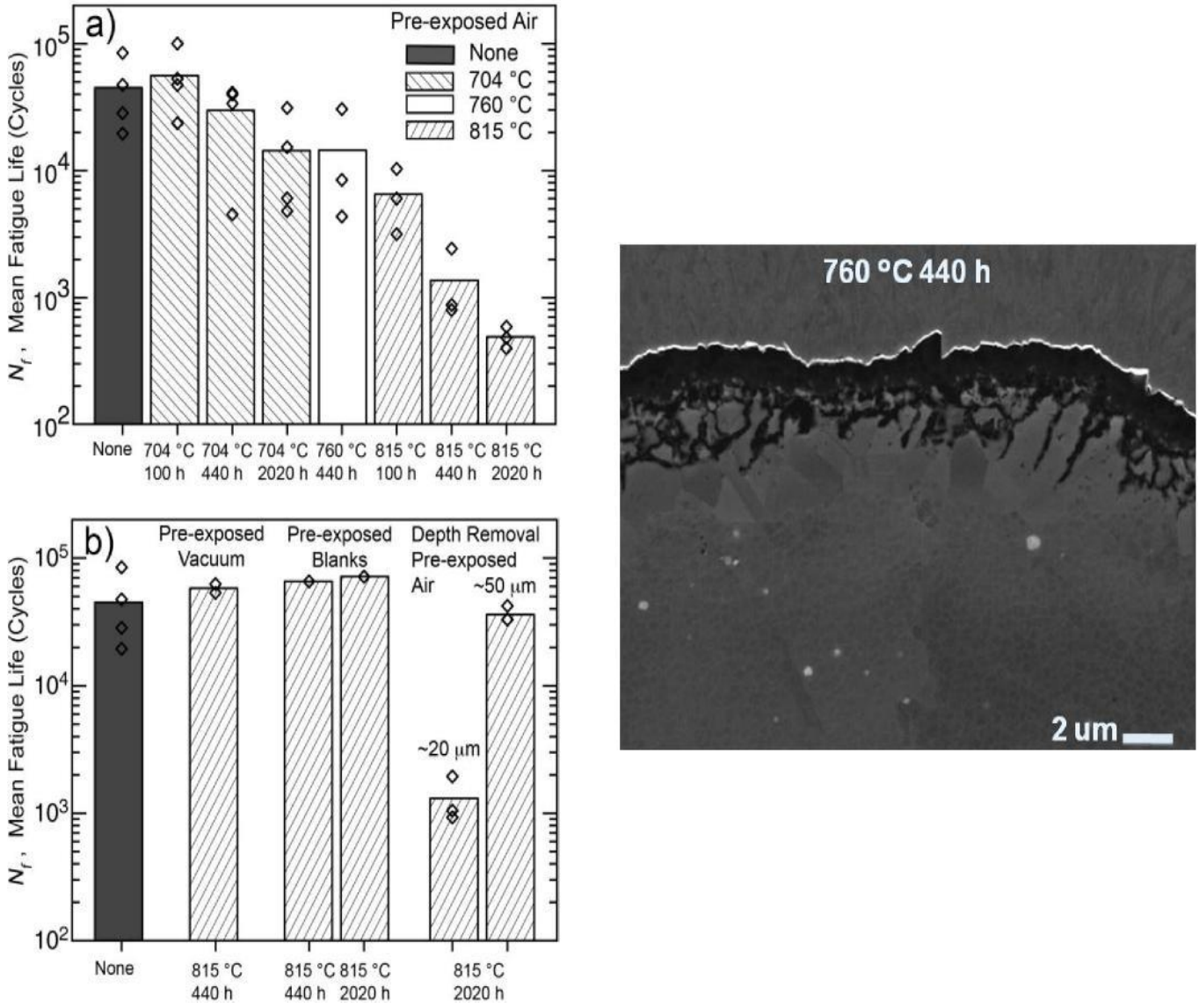

Figure 11. Comparison of the mean notched fatigue lives at 704°C of the unexposed ME3 specimens and ME3 specimens with a) prior exposures in air and b) alternate conditions as marked (Misra, 2012).

because of quick crack propagation that could ultimately cause the specimen to fracture. Based on this assumption, at temperatures 650, 704 and 760°C, fracture could occur at 5000, 6500, and 650 cycles respectively. By using these three boundary conditions, a convex curve is developed and indicated in Table 9. This experiment is conducted at maximum force. By solving the equation (convex curve) in Table 9 at condition, N=0, maximum temperature that is allowed to work in maximum mechanical force, 763°C, is

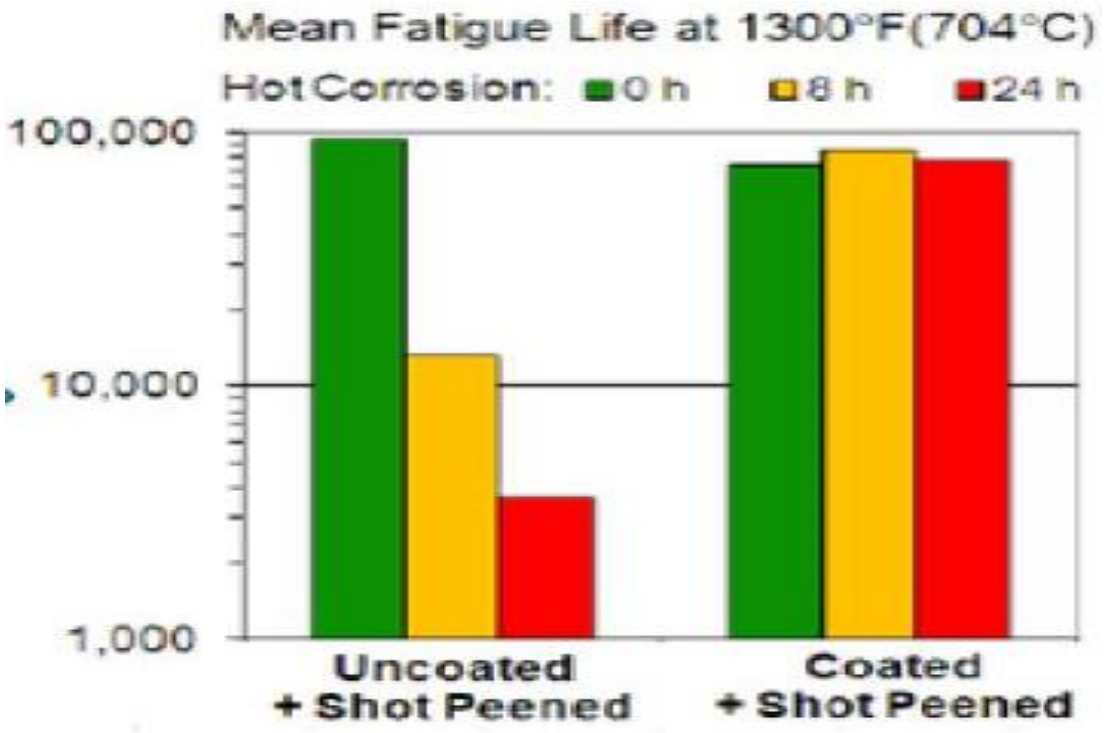

Figure 12. Effectiveness of coating in providing hot corrosion protection for ME3 disk alloy (Misra, 2012).

Table 8. Boundary conditions and fatigue life equations that are as functions of time and temperature at different conditions.

ME3	Boundary Conditions (Misra, 2012)	Equation
at 704°C	(*t*=100 h, *N*=5.5e+4 Cycles), (*t*=440 h, *N*=3e+4 Cycles), and (*t*=2020 h, *N*=1.4e+4 Cycles) (Figure 11)	$0.03302(t^2)-91.36144(t)+63805.94418=N$, (33) *Concave Curve*
at t=440 h	(*T*=704°C, *N*=30000 Cycles), (*T*=760°C, *N*=14000 Cycles), and (*T*=815°C, *N*=1300 Cycles) (Figure 11)	$0.49374(T^2)-1008.54966(T)+495313.5168=N$, (34) *Concave Curve*
at t=2020 h	(*T*=704°C, *N*=14000 Cycles) and (*T*=815°C, *N*=400 Cycles) (Figure 11)	$100255.8559-122.5225(T)=N$, (35) *Linear*
T=704°C, Coated+Shot Peened	(*t*=0 h, *N*=7.1e+4 Cycles), (*t*=8 h, *N*=8.5e+4 Cycles), and (*t*=24 h, *N*=7.5e+4 Cycles) (Figure 12)	$-98.95833(t^2)+2541.6667(t)+71000=N$, (36) *Convex Curve*
T=704°C, Uncoated+Shot Peened	(*t*=0 h, *N*=9.6e+4 Cycles), (*t*=8 h, *N*=1.4e+4), and (*t*=24 h, *N*=3400) (Figure 121)	$399.4792(t^2)-13445.8333(t)+96000=N$, (37) *Concave Curve*
T=704°C, Uncoated+Shot Peened	(*t*=0 h, *N*=9.6e+4 Cycles) and (*t*=8 h, *N*=1.4e+4 Cycles) (Figure 12)	$-10250(t)+96000=N$, (38) *Linear*
T=704°C, Uncoated+Shot Peened	(*t*=8 h, *N*=1.4e+4 Cycles) and (*t*=24 h, *N*=3400 Cycles) (Figure 12)	$-662.5(t)+19300=N$, (39) *Linear*

Table 9. Fatigue life boundary conditions and equation in gas turbine engine at maximum force as a function of temperature variation.

ME3	Boundary Conditions (Maciejewski, 2013)	Equation
At Maximum Force	(T=650°C, N=5000 Cycles), (T=704°C, N=6500 Cycles), and (T=760°C, N=650 Cycles), (Figure 4)	$1.2022(T^2)+1655.55792(T)-563183.1472=N$, (40) *Convex Curve*

Table 10. Specimen and fatigue test conditions with mean life results.

Machining condition	Corrosion time (h)	Test temperature (°C)	Log mean life cycles
Low Stress Ground	0	204	147,924
Low Stress Ground	8	204	57,175
Low Stress Ground	24	204	34,616
Shot Peened	0	204	254,527
Shot Peened	8	204	250,908
Shot Peened	24	204	75,921
Low Stress Ground	0	704	80,099
Low Stress Ground	8	704	3,768
Low Stress Ground	24	704	1,970
Shot Peened	0	704	92,936
Shot Peened	8	704	13,202
Shot Peened	24	704	3,616

Source: Gabb et al. (2009).

achieved. Thus, it appears that at maximum force in gas turbine engine, temperature always has to be less than 763°C. In the following parts of this research, this method is repeatedly used and critical temperatures and times allowed to use ME3 at different environments are achieved.

ME3 failure time at 204 and 704°C

Many experiments are performed by NASA to determine the ME3 super alloy fatigue life. Results from one of these experiments are indicated in Table 10 (Gabb et al., 2009). These results are classified at both 204 and 704°C in low stress ground and shot peened ME3. The experiments are performed at 0, 8, and 24 h exposure to 204 and 704°C, and gas turbine engine different conditions. At each of these exposure times, the fracture cycle number or fatigue life is determined. By using these experimental data in Table 10 (Gabb et al., 2009), numbers of equations to predict the ME3 maximum lifetime of exposure are developed and indicated in Table 11. Many results for ME3 maximum lifetime of exposure is achieved by these functions, but it is important to notice that because at 24 h exposure, ME3 still has a remaining life, the ME3 lifetime must be more than 24 h. For Table 11 data interpretation, the procedure that has previously been used, is repeated.

ME3 failure results

Previously, in this paper, the aim has been for developing equations to predict the maximum lifetime and temperature allowed for ME3 at different environments of aerospace gas turbine engines. Here, these functions are solved and the critical numerical values of times and temperatures are achieved. These critical and vital numerical values are presented in Tables 12 and 13.

In Tables 12 and 13, all the information related to temperature and time limit in ME3 at gas turbine engines is indicated. These data are achieved by the convex, concave, and linear functions method. By reviewing Table 12, two significant and vital data are presented. This information is related to two critical temperatures, 773 and 763°C. These temperatures are the minimum numerical values of temperatures in Table 12 that limit the temperature allowed for use in ME3 super alloy at aerospace gas turbine engines. These data prove that at 773°C in relation to the 0.00375 strain at gas turbine engine, the yield strength is equal to yield stress. Thus, ME3 at disks and blades could yield at this temperature. This could end up in crashing to other adjacent parts of gas turbine like body and shaft. It may also lead to disallowed deformation of blades and disks that finally could result in gas turbine structural damage. This damage could be due to crack initiation and propagation, and ultimately fracture because of insufficient yield strength.

However, based on this method, it seems logical to keep the ME3 temperature at gas turbine engine always below the 763°C.

By comparing between rows 8 and 9 in Table 12, it can be observed that by increasing the ME3 exposure time from 440 to 2020 h (359.09% increase), the temperature limit decreases form 821 to 818°C. This is interpreted as 0.37% decrease in temperature limit due to ME3 fatigue life.

The salt mixture, applied in a ring around the middle of the gage section, melted at 704°C and caused pits to form within and along the edges of this ring. The 8 h corrosion exposure produced fewer, usually separated pits that were near hemispherical in profile, as indicated by the arrows. The 24 h exposure produced a higher density of pits, which were sometimes joined together along the ring edges, also indicated. The range of pit morphologies captured by 8

Table 11. Boundary conditions for obtaining ME3 maximum life time equations at different conditions.

ME3	Boundary conditions (Gabb et al., 2009)	Equation
At 704°C, Low Stress Ground	(t=0 h, N=80099 Cycles), (t=8 h, N=3768 Cycles), and (t=24 h, N=1970 Cycles) [Table 10]	392.875(t^2)-12684.375(t)+80099=N, (41) *Concave Curve*
At 704°C, Shot Peened	(t=0 h, N=92936 Cycles), (t=8 h, N=13202 Cycles), and (t=24 h, N=3616 Cycles) [Table 10]	390.31771(t^2)-13089.29167(t)+92936=N, (42) *Concave Curve*
At 204°C, Shot Peened	(t=0 h, N=254527 Cycles), (t=8 h, N=250908 Cycles), and (t=24 h, N=75921 Cycles) [Table 10]	-436.8464(t^2)+3042.396 (t)+254527=N, (43) *Convex Curve*
At 704°C, Low Stress Ground	(t=0 h, N=80099 Cycles) and (t=24 h, N=1970 Cycles) [Table 10]	-3255.375(t)+80099=N, (44)
At 704°C, Low Stress Ground	(t=8 h, N=3768 Cycles) and (t=24 h, N=1970 Cycles) [Table 10]	-112.375(t)+4667=N, (45)
At 704°C, Shot Peened	(t=0 h, N=92936 Cycles) and (t=8 h, N=13202 Cycles) [Table 10]	-9966.75(t)+92936=N, (46)
At 704°C, Shot Peened	(t=8 h, N=13202 Cycles) and (t=24 h, N=3616 Cycles) [Table 10]	-599.125(t)+17995=N, (47)

Table 12. ME3 failure temperature at different conditions obtained by the equations in "*Problem Formulation*" of the present research.

1	Equation name	Functions	Critical functions	ME3 Failure Temp. (°C)
2	T-S_u, Fine ME3	$-0.4741(T)+1631.85185=S_u$, (28)	If S_u=E.ε=922.5 MPa	1496
3	T-S_u, Course ME3	$-0.00361(T^2)+2.11222(T)+1599.45083=S_u$, (30)	If S_u=E.ε=922.5 MPa	815
4	T-S_y, Fine ME3	$-0.2074(T)+1185.1852=S_y$, (27)	If S_y=E.ε=922.5 MPa	1266
5	T-S_y, Course ME3	$-0.00071(T^2)+0.26285(T)+1143.8725=S_y$, (29)	If S_y=E.ε=922.5 MPa	773
6	T-S_u, ME3	$-0.002065(T^2)+0.94057(T)+1627.7764=S_u$, (31)	If S_u=E.ε=922.5 MPa	854
7	T-S_t, ME3	$-0.00341(T^2)+1.85847(T)+1664.1946=S_t$, (32)	If S_t=E.ε=922.5 MPa	812
8	T- N_f, ME3	Exposure Time=440 h, $0.49374(T^2)-1008.54966(T)+495313.5168=N_f$, (34)	If N_f = 0	821
9	T- N_f, ME3	Exposure Time=2020 h, $100255.8559-122.5225(T)=N_f$, (35)	If N_f = 0	818
10	T- N_f, ME3	$-1.2022(T^2)+1655.55792(T)-563183.1472=N_f$, (40) Maximum force condition	If N_f = 0	763*

and 24 h exposures allowed determination of how variations in pit characteristics influence fatigue life (Gabb et al., 2009).

According to Table 13, the most crucial condition for ME3 is in 704°C and low stress ground because it offers the minimum lifetime

Table 13. ME3 failure time at different conditions obtained by the equations in "*Problem Formulation*" of the present research.

1	Equation name	Functions	Critical functions	Failure Time
2	Coated + Shot Peened ME3 at 704°C	$-98.9583(t^2)+2541.6667(t)+71000=N_f$, (36)	If $N_f=0$	42 h + 32 min
3	Uncoated + Shot Peened ME3 at 704°C	$399.4792(t^2)-13445.8333(t)+96000=N_f$, (37)	If $N_f=0$	10 h +16 min Not Accepted
		$-10250(t)+96000=N_f$, (38)		9 h + 21 min Not Accepted
		$-662.5(t)+19300=N_f$, (39)		29 h + 7 min **Accepted**
4	Shot Peened ME3 at 704°C	$390.3177(t^2)-13089.2917(t)+92936=N_f$, (42)	If $N_f=0$	10 h +12 min 23 h +19 min Not Accepted
		$-9966.75(t)+92936=N_f$, (46)		9 h+19 min Not Accepted
		$-599.125(t)+17995=N_f$, (47)		30 h+2 min **Accepted**
5	Low Stress Ground ME3 at 704°C	$392.875(t^2)-12684.375+80099=N_f$, (41)	If $N_f=0$	8 h +36 min 23 h+ 40 min Not Accepted
		$-3255.375(t)+80099=N_f$, (44)		24 h+36 min **Accepted**
		$-112.375(t)+4667=N_f$, (45)		41 h+31 min Not Accepted
6	Shot Peened ME3 at 204°C	$-436.8464(t^2)+3042.396(t)+254527=N_f$, (43)	If $N_f=0$	27 h +52 min
7	ME3 at 704°C	$0.03302(t^2)-91.36144(t)+63805.94418=N_f$, (33)	If $N_f=0$	No Result

of 24 h and 36 min. In conditions that the ME3 super alloy is shot peened and the temperature is 204°C, the ME3 lifetime is 27 h and 52 min. This increase in ME3 lifetime is due to shot peened and lower temperature in comparison with 704°C condition. The minimum result of ME3 lifetime for shot peened and 704°C is 29 h and 7 min. As a result, in this condition the ME3 exposure time must always be less than this time. Coated and shot peened ME3 at 704°C is the most efficient ME3. In this condition, it can perform to maximum 42 h and 32 min as did the ME3 maximum lifetime of exposure in gas turbine engine. Thus, based on the results indicated in Table 13, the worst condition for ME3 is low stress ground at 704°C and best state is coated and shot peened ME3 at 704°C. By comparing between the worst ME3 condition (low stress ground at 704°C), and the shot peened ME3 at 204°C, the shot peened at 704°C, and coated and shot peened at 704°C; increase in maximum lifetime of exposure in gas turbine engine occurs at 13.25, 18.33 and 72.88%, respectively.

The effect of coating on shot peened ME3 maximum exposure lifetime at 704°C is measured with the data in Table 13. This can increase the maximum lifetime from 29 h and 7 min to 42 h and 32 min that is interpreted as 46.1% increase in maximum exposure lifetime.

RESULTS

In the present part of this research, the results that are obtained from the *"ME3 fatigue life in gas turbine"* part of the present paper for ME3 super alloy crack density are compared with other experiment crack density. In gas turbine engine, ME3 is under mechanical cyclic load with the amplitude of $\Delta\sigma_2=E.\varepsilon$=(246e+9).(7.5e-3)=1845 MPa (Gabb et al., 2009) and in the other experiment for $[0_2/90_4]$ Fiberite 934/T300 composite, mechanical cyclic load amplitude is $\Delta\sigma_1$=188.4 MPa (Liu and Nairn, 1990). In Table 14, crack density comparison at 0, 1000, and 5000 Cycles between $[0_2/90_4]$ Fiberite 934/T300 composite material under mechanical cyclic load (Liu and Nairn, 1990) and ME3 super alloy under mechanical cyclic load at 704°C, is indicated.

According to comparison between $[0_2/90_4]$ Fiberite 934/T300 average crack density and ME3 average crack

Table 14. Crack density comparison at 0, 1000, and 5000 Cycles between $[0_2/90_4]$ Fiberite 934/T300 composite material under mechanical cyclic load (Liu and Nairn, 1990) and ME3 super alloy under mechanical cyclic load at 704°C.

Cycles	0	1000	5000
$[0_2/90_4]$ Fiberite 934/T300 Crack Density (mm^{-1}) (Liu and Nairn, 1990)	0	0.13	0.17
ME3 Crack Density (mm^{-1})	0	0.375	3.667
$[0_2/90_4]$ Fiberite 934/T300 Average Crack Density, $D_{Ave,1}$ (mm^{-1})		0.1	
ME3 Average Crack Density, $D_{Ave,2}$ (mm^{-1})		1.3475	

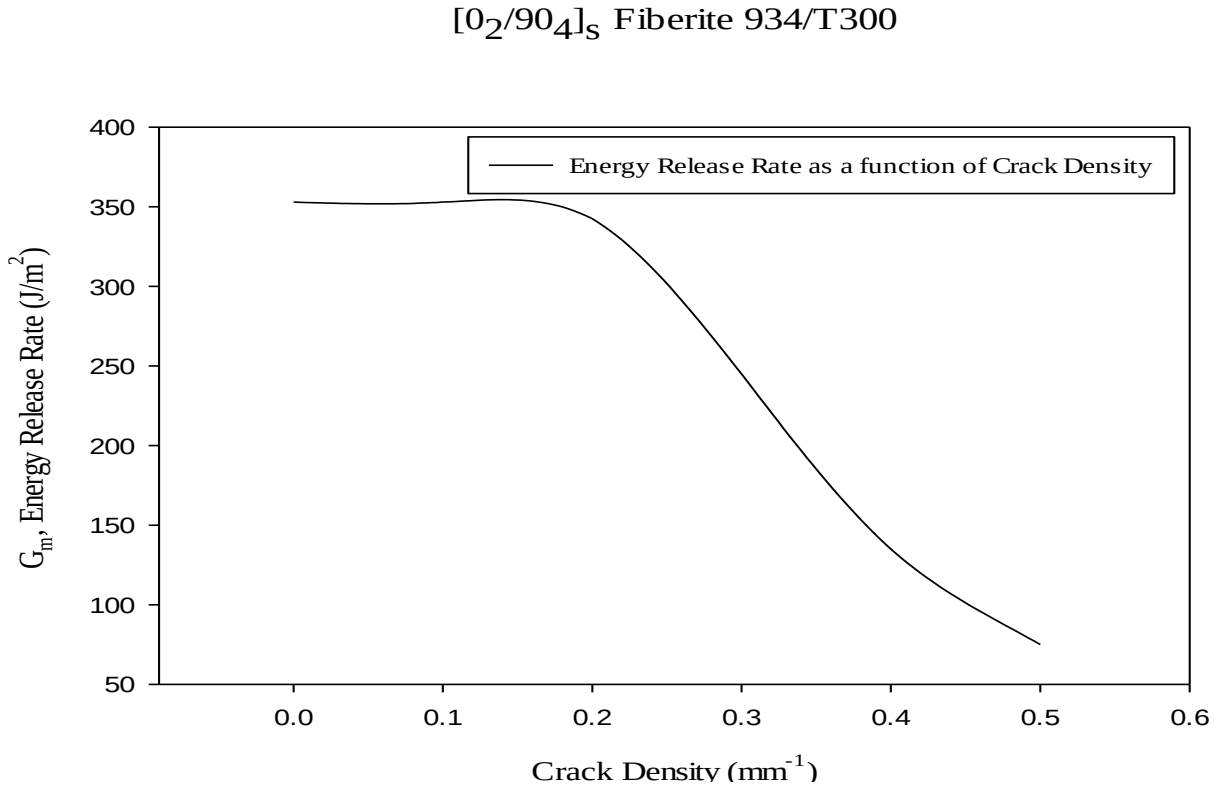

Figure 13. Energy release rate as a function of crack density for $[0_2/90_4]$ Fiberite 934/T300 composite in fatigue life experiment under mechanical cyclic load $\Delta\sigma_1$=188.4 MPa (Liu and Nairn, 1990).

density, it seems that Relation (48) is correct. The difference between the stress cyclic load proportion (left side of Relation (48)) and average crack density proportion (right side of Relation (48)) is about 27.4%. In Figures 13 and 14, energy release rate as a function of crack density for $[0_2/90_4]$ Fiberite 934/T300 and ME3 is illustrated respectively. Furthermore, Figure 15 shows, crack density growth rate as a function of energy release rate for $[0_2/90_4]$ Fiberite 934/T300.

$$\frac{\Delta\sigma_1}{\Delta\sigma_2} \cong \frac{D_{Ave,1}}{D_{Ave,2}}, \qquad (48)$$

$$0.1022 \cong 0.0742.$$

DISCUSSION

By considering the results of this study, it appears that the margin of safety for ME3 in aerospace gas turbine engines is determined by the methodology presented. This margin of safety is defined by the numbers of values for critical temperature, stress, force cycles, and exposure time.

In the results that are obtained by this study, it appears that as temperature, stress, numbers of force cycles, and exposure time increases, ME3 mechanical properties deteriorates and get closer to failure. It seems that the cause for this deterioration might be due to change in ME3 nanostructure. As temperature, stress, force cycles, and exposure time of ME3 increase, it seems that, it

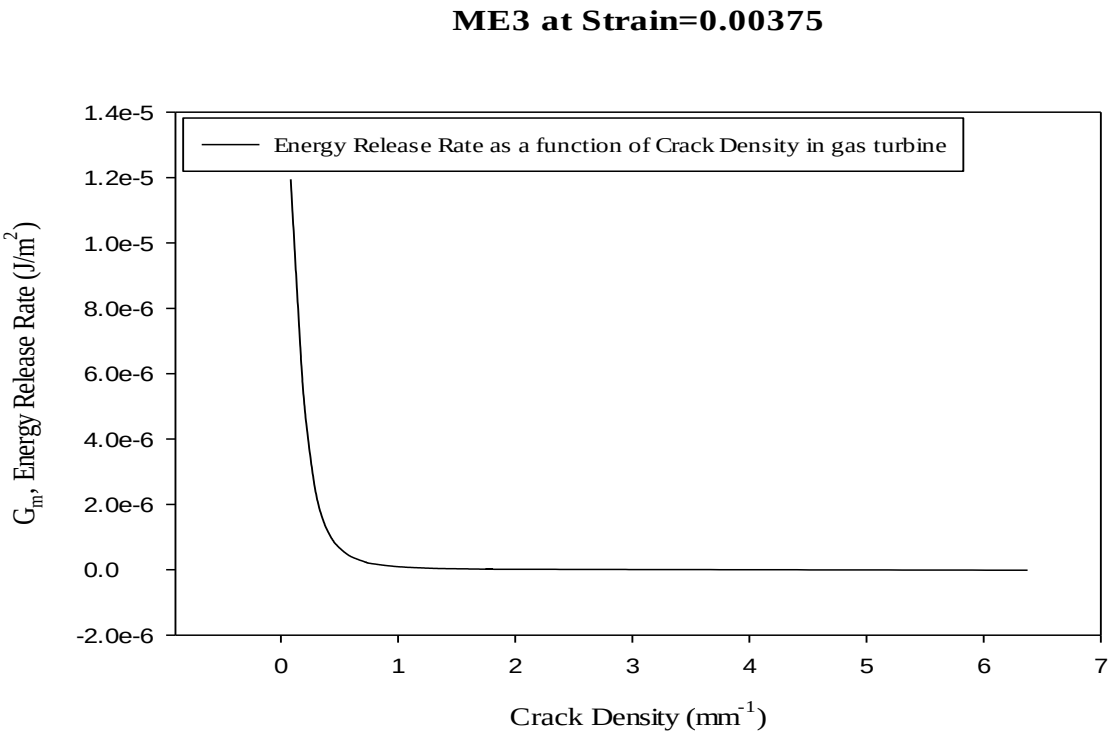

Figure 14. Energy release rate as a function of crack density for 6 mm thickness ME3 super alloy in fatigue life experiment at 704°C under mechanical cyclic load $\Delta\sigma_2$=1845 MPa in aerospace gas turbine engine environment simulation experiment.

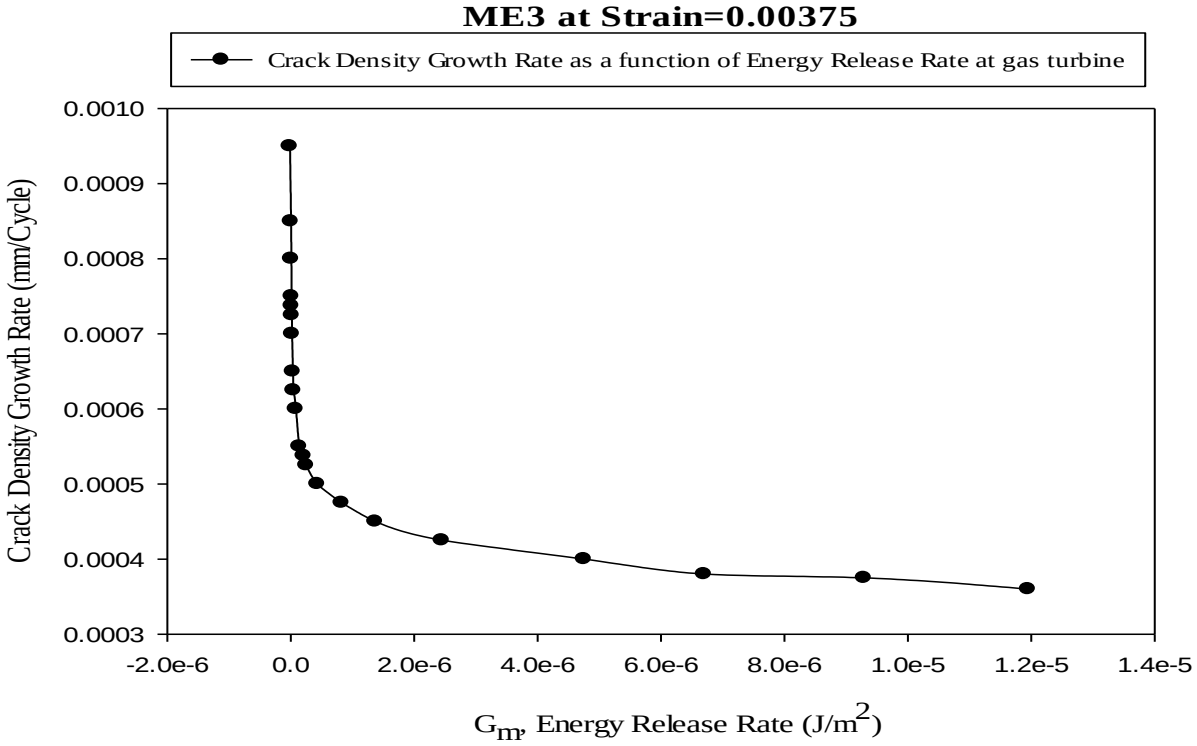

Figure 15. Crack density growth rate as a function of energy release rate for 6 mm thickness ME3 super alloy in fatigue life experiment at 704°C under mechanical cyclic load $\Delta\sigma_2$=1845 MPa in aerospace gas turbine engine environment simulation experiment.

causes the distance between the ME3 nano particles to increase until it reaches the threshold value that may cause failure in ME3 super alloy.

Conclusions

In the presented study, by using analytical solutions and applying experimental data, equations to predict the ME3 life in gas turbine engine environment simulation are obtained. ME3 is one of the Nickel-base super alloys that is applied in aerospace gas turbine engines and is subjected to high temperatures over 700°C. The results of this method are compared with the data by another mechanical cyclic load fatigue experiment. The comparison has shown that the ME3 fatigue life prediction seems correct. Ultimately, the results achieved by convex, concave, and linear equations indicated the maximum exposure time and temperature allowed for ME3 at different conditions in aerospace gas turbine engines such as elevated temperatures along with the use of coating for ME3. As it appears, results has proved that, at maximum mechanical engine power the ME3 temperature must always be below 763°C. In addition, it may be concluded that at engine normal condition, the temperature must never be as high as 773°C, which is the failure temperature. Based on these results, it is recommended that coated and shot peened ME3 be used at gas turbine. This fact is of high importance because it can increase the ME3 exposure lifetime at aerospace gas turbine engines up to 72.88%. For the future work, creep failure prediction of ME3 super alloy in aerospace gas turbine engines is highly recommended.

CONFLICT OF INTERESTS

The author has not declared any conflict of interests.

ACKNOWLEDGEMENTS

The author would like to appreciate the guidance of advisors. All the funding related to this research is provided by the presented author.

Symbols

E: Elasticity Modulus
σ_f: Strength
b: Constant
c: Constant
$\Delta\varepsilon$: Strain range
ε_f: Strain strength
$2N_f$: Crack initiation life cycles
E_A: Axial moduli
E_T: Transverse moduli
T_s: Specimen temperature
T_0: Stress free temperature
$\Delta\alpha$: Difference between the transverse and longitudinal thermal expansion coefficients
α_T: Transverse thermal expansion coefficient
α_A: Longitudinal thermal expansion coefficient
p, q, α, β, C_1, C_2, C_3, C_4: Constants function of mechanical properties and thickness of material
t: Material thickness
h: Composite material thickness
B: Twice the composite material thickness
G_A: Axial shear moduli
G_T: Transverse shear moduli
υ_A: Axial Poisson's ratio
υ_T: Transverse Poisson's ratio
W: Specimen width
L: Sample length
2a: Distance between two cracks
C_W: Crack's width
G_m: Energy release rate
$\chi(\rho)$: Material properties function
Y(D): Calibration function
D: Crack density
A: Power-law fitting parameter
n: Power-law fitting parameter
ΔK: Applied stress intensity factor
N_c: Crack numbers
a_c: Crack length

REFERENCES

Adair BS (2013). Characterization and modeling of thermo-mechanical fatigue crack growth in a single crystal superalloy, Ph.D. thesis, Georgia institute of technology, USA.
Anvari A (2014). Fatigue life prediction of unidirectional carbon fiber/epoxy composite in earth orbit. Int. J. Appl. Math. Mech. 10(5):58-85.
Anvari A (2016). Friction coefficient variation with sliding velocity in copper with copper contact. Periodica Polytech. Mech. Eng. 60(3):137-141.
Anvari A (2017). Crack growth as a function of temperature variation in carbon fiber/epoxy. J. Chem. Eng. Mater. Sci. 8(3):17-30.
Anvari A (2017a). Effect of nano-carbon percentage on properties of composite materials. J. Chem. Eng. Mater. Sci. 8(4):31-36.
Anvari A (2017b). Fatigue life prediction of unidirectional carbon fiber/epoxy composite on Mars. J. Chem. Eng. Mater. Sci. Under press.
Adibnazari S, Anvari A (2017). Frictional effect on stress and displacement fileds in contact region. J. Mech. Eng. Res. 9(4):34-45.
Assoul Y, Benbelaid SV, Zeravcic VS, Bakic G, Dukic M (2008). Life estimation of first stage high pressure gas turbine blades. Scientific Technical Rev. 58(2):8-13.
Basan R, Franulovic M, Krizan B (2010). On estimation of Basquin-Coffin-Manson fatigue parameters of low-alloy steel AISI4140, 14th International Research/Expert Conference "Trends in the development of machinery and associated technology", (TMT 2010, Mediterranean Cruise). pp. 453-456.
Bhattacharjee A (2013). Elastostatic problem of a series of collinear cracks in an orthotropic medium. Int. J. Appl. Math. Mech. 9(20):81-97.
Chen DC, You CS (2015). Fracture criterion for the tensile test of 7075 aluminum allo. J. Strength Mater. 47(1):122-127.

El-Sayed AF (2017). Aircraft Propulsion and Gas Turbine Engines, (CRC Press, Taylor & Francis Group. P 496.
Gabb P, Telesman J, Hazel B, Mourer DP (2009). The effects of hot corrosion pits on the fatigue resistance of a disk superalloy, Glenn research center, Cleveland, Ohio[1], GE Aviation, Cincinnati, Ohio[2], GE Aviation, Lynn, Massachusetts[3].
Gabb P, Telesman J, O'Connor K, Kantzos PT (2002). Characterization of the temperature capabilities of advanced disk alloy ME3, Glenn Research Center, Cleveland, Ohio[1], Ohio aerospace institute, Brook park, Ohio[2].
Gao Y, Kumar M, Nalla RK, Ritchie RO (2005). High-cycle fatigue of Nickel-based superalloy ME3 at ambient and elevated temperatures: role of grain-boundary engineering. Metallurg. Mater. Transactions A, 36A:3325-3329.
Gao Y, Stolken JS, Kumar M, Ritchie RO (2007). High-cycle fatigue of nickel-base super alloy Rene 104 (ME3): Interaction of microstructurally small cracks with grain boundaries of known character, Acta Materialia. 55:3155-3167.
Getsov LB, Semenov AS, Semenov SG, Tikhomirova EA, NPO CKTI, Saint-Petersburg state polytechnical university and JSK Klimov (2014). Experiments and failure criteria for single crystal alloys of gas turbine engine under static and thermocyclic loading, 29th Congress of the International Council of the Aeronautical Sciences, (St Petersburg, Russia, pp. 1-6.
Jiang R, Everitt S, Gao N, Soady K, Brooks JW, Reed PAS (2015). Influence of oxidation on fatigue crack initiation and propagation in turbine disc alloy N18, Materials research group.
Liu S, Nairn JA (1990). Fracture mechanics analysis of composite microcracking: experimental results in fatigue, in Proceeding of the 5th Technical Conference on Composite Materials, American Society of Composites, (East Lansing, Michigan). pp. 287-295.
Maciejewski K (2013). The role of microstructure on deformation and damage mechanisms in a Ni-based superalloy at elevated temperatures, Ph.D. thesis, University of Rhode Island.
Misra A (2012). Durability challenges for next generation of gas turbine engine material, NASA Glenn research center, Cleveland, OH 44134.
Nembach E, Neite G (1985). In progress in materials science (ed Christian JW, Haasen P, Massalski TB). Pergamon press Oxford 29:177.
Roy SS, De J (2014). Interfacial crack problems in dissimilar bonded materials. Int. J. Appl. Math. Mech. 10(7):16-27.
Sawant A, Tin S, Zhao JC (2008). High temperature nanoindentation of ni-base super alloys, TMS (The Minerals, Metals & Materials Society).
Winston MR, Brooks JW (2008). Advanced high temperature materials: aeroengine fatigue, Physical sciences department, defence science and technology laboratory, Porton Down, Salisbury, SP4 0JQ, UK[1], QinetiQ Ltd., Cody Technology Park, Farnborough, GU14 0LX, UK[2].
Xue F, Yu WW, Yu M, Liu W, Shu GG (2015). Long-term aging effect on the crack growth in the main circulating pump casing material. J. Strength Mater. 47(1):100-107.
Yang B, Ma BQ, Zhao YX, Xiao SN (2015). Short fatigue crack growth at different maintenance times for LZ50 steel. J. Strength Mater. 47(1):114-121.
Zaretsky EV, Litt JS, Hendricks RC, Soditus SM (2012). Determination of turbine blade life from engine field data, NASA Glenn researchcenter, Cleveland, Ohio 44135[1], United airlines maintenance, San Francisco, California 94128[2].